Journal of Polymers and the Environment (2021) 29:1143–1152
https://doi.org/10.1007/s10924-020-01950-1

ORIGINAL PAPER

Preparation and characterization of gelatin/β-glucan nanocomposite film incorporated with ZnO nanoparticles as an active food packaging system

Shahin Sherafatkhah Azari[1] · Ainaz Alizadeh[1] · Leila Roufegarinejad[1] · Narmela Asefi[1] · Hamed Hamishehkar[2]

Accepted: 22 October 2020 / Published online: 31 October 2020

Abstract

In this study, nanocomposite film as biodegradable active packaging was fabricated by incorporation of gelatin and β-glucan (0, 10, and 20% w/w) in the presence of ZnO nanoparticles (0, 2.5, and 5% w/w); further, it was characterized by XRD, DSC, SEM, and FT-IR analyses. The obtained results exhibited that the incorporation of ZnONPs and β-glucan had no adverse effect on the morphological and thermal properties and the crystallinity of gelatin-based films, indicating appropriate interaction and good compatibility between gelatin matrix, ZnONPs, and β-glucan. Moreover, the increasing concentrations of β-glucan and ZnONPs increased strain to break and the ultimate tensile strength of film samples. The film samples containing a high concentration of ZnONPs showed higher water barrier properties (moisture absorption and water vapor permeability) and surface hydrophobicity. Additionally, the incorporation of ZnONPs in the film samples provided high antibacterial activity against foodborne pathogenic bacteria. In conclusion, the ZnONPs and β-glucan incorporated gelatin-based nanocomposite film could be applied as an active food-packaging system due to its unique features.

Graphic Abstract

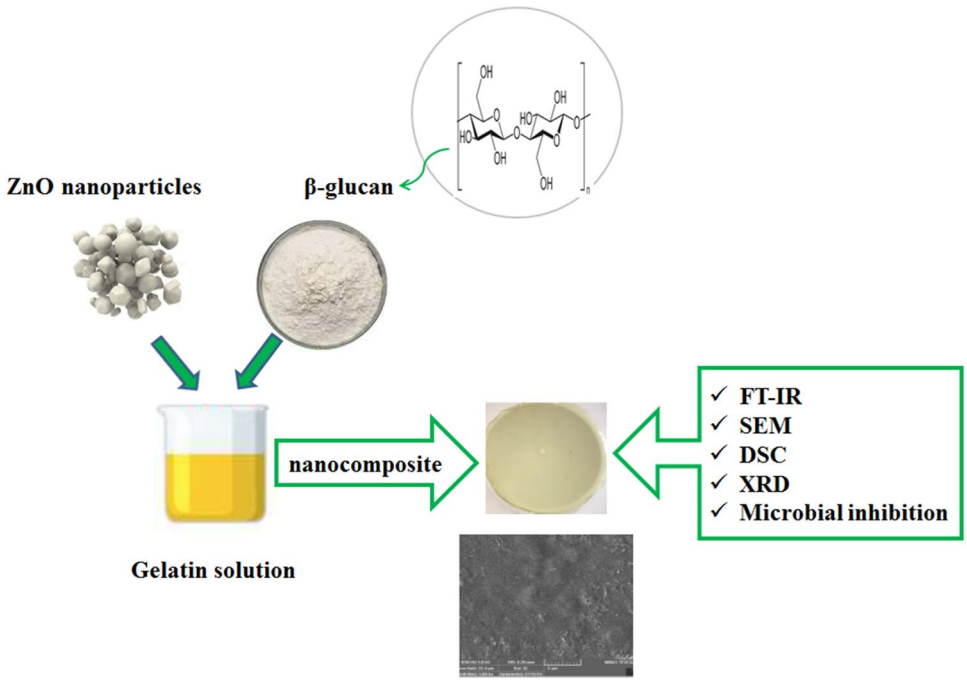

Keywords Biodegradable packaging · Biopolymers · Antibacterial activity · Gelatin

Extended author information available on the last page of the article

Introduction

Biodegradable packaging has become an icon in the packaging industry; it plays a vital role in modern society. The key functions of food packaging are to preserve the food products and extend their shelf life until consumption [1]. Biodegradable packaging based on edible films, mainly made of polysaccharides, proteins, lipids, or their combination, is vital in the packaging industry [2, 3]. These polymers have some interesting properties, including the ability to be renewed and the absence of environmental pollution, that make them so important [4]. Gelatin as a biopolymer is widely used in food, cosmetic, pharmaceutical, medical, and agriculture technologies due to its biodegradability in physiological environments [5]. Furthermore, it is an interesting biopolymer to be applied in the production of biodegradable films due to its favorable properties, such as good film-forming ability, abundancy, good oxygen barrier capacity, as well as low gelling and melting points [5, 6]. However, gelation-based films' poor water barrier, besides their thermal and mechanical properties, restrict their application in food packaging [7]. To overcome these limitations, the combination of gelatin with other biopolymers, especially carbohydrates, is suggested, being called "composite films" [1]. β-Glucan is a polysaccharide synthesized by plant and microbial resources [8]. The rheologicality, biocompatibility, biodegradability, and film-forming ability in β-glucan make it an interesting biopolymer in film production [9]. Moreover, it has health benefits, such as decreasing blood lipid levels, besides balancing blood pressure, blood glucose, and insulin response [10]. In recent years, the incorporation of nanoparticles (NPs) into composite materials has attracted a great deal of attention due to its ability to enhance the thermal, mechanical, and gas barrier properties of polymers [11]. Some metal oxide NPs, such as zinc oxide (ZnO), titanium dioxide (TiO_2), magnesium oxide (MgO), and silicon dioxide (SiO_2) NPs, act as antibacterial agents besides their ability to block UV radiation [12]. ZnONPs are one of the best and safest nanoparticles to be applied in food packaging [13]. They are low cost and easily available with antibacterial effects and intensive ultraviolet absorption [14]. Furthermore, ZnONPs have been approved by the FDA as safe materials [15]. In this regard, ZnONPs have been recently incorporated into a number of different polymers to improve the antibacterial properties of the packaging materials [2, 4, 12, 16]. According to the literature review, there is no study on the combination of gelatin and β-glucan to produce a double base biopolymer nanocomposite film to compensate for gelatin deficiencies in film. Therefore, this study aims to prepare and characterize ZnONPs incorporated gelatin/β-glucan nanocomposite, analyzing the gelatin and β-glucan interaction in the film matrix to apply as a novel biodegradable active packaging system.

Materials and Method

Materials

Gelatin (medium molecular weight and 99% purity) was obtained from Sigma-Aldrich (St. Louis, USA). Zinc oxide powder with a purity of 99.99% and particle size of 40 nm were purchased from the Iranian Nanomaterials Pioneers Co. (Mashhad, Iran). Yeast β-Glucan was obtained from Soren Tak Toos Co. (Mashhad, Iran). Glycerol (with 99.5% (W/W) purity), were provided from Charles Co. (Spain). Different salts, used to prepare saturated solutions to provide desired relative humidity (RH) were received from Merck Chemicals Co (Darmstadt, Germany).

Preparation of Nanocomposite Film

Firstly, 4 g of gelatin powder was dissolved in 100 mL of distilled water at 45° C and stirred for 30 min. The glycerol (2 mL) was then added to the film solution and stirred at 45° C for 15 min. Then, ZnONPs (0, 2.5 and 5% w/w) were dispersed in 50 mL of distilled water and sonicated (80 W) for 5 min. Subsequently, the NPs solution is gradually added to 50 mL of gelatin solution and placed on a magnetic stirrer for 30 min at 600 rpm. Different percentages of β-Glucan (0, 10 and 20% w/w) were dissolved in 30 ml of distilled water and mixed with 70 mL of the film solution and was stirred for 10 min using a magnetic stirrer. After that, 80 ml of the prepared solution was poured onto a polypropylene plate and dried at 40 °C for 24 h in a drying oven at ambient RH [17]. The prepared film samples are presented in Table 1.

Table 1 The prepared gelatin-based film samples

Sample code	Gelatin (%)	β-Glucan (%)	ZnONPs (%)
G	100	0	0
G/βG10%	90	10	0
G/βG20%	80	20	0
G/ZnONPs2.5%	97.5	0	2.5
G/βG10%/ZnONPs2.5%	87.5	10	2.5
G/βG20%/ZnONPs2.5%	77.5	20	2.5
G/ZnONPs5%	95	0	5
G/βG10%/ZnONPs5%	85	10	5
G/βG20%/ZnONPs5%	75	20	5

G gelatin; *βG* β-glucan and *ZnONPs* zinc oxide nanoparticles

Characterization of Films

Thickness Measurement

The thickness of the films was measured by a digital micrometer (Alton m820-25, China) with a precision of 0.01 mm at 10 random points of the film. The average thickness of each film was used to calculate mechanical properties and water vapor permeability [18].

Measurement of Moisture Absorption

Neus Angle`s & Dioufers [19] method was used to measure the moisture absorption of the films. The film samples (2 × 2 cm) were placed in a desiccator containing calcium sulfate (RH = 0%) for 24 h. After initial weighing, the samples were transferred to a desiccator containing sodium chloride saturated solution (RH = 75%) and stored at 20 to 25 °C. Then, all samples were weighed at different times until constant weight by sensitive scales, and the moisture absorption was calculated from the ratio of:

$$\text{Moisture absorption } (\%) = \frac{Wt - W0}{W0} \times 100 \quad (1)$$

where, Wt and W0 are the initial weight and final weight of the film samples, respectively.

Water Vapor Permeability (WVP) Measurement

WVP of film was measured using ASTM E 96–95 method. For testing, vials with a diameter of 20 mm and a depth of 45 mm were used. The films (2 × 2 cm) were placed in the vials containing 3 g of calcium sulfate. After initial weighing, the vials were placed in a glass desiccator containing potassium sulfate (97% RH), and then the amounts of vapor transferred from the film were determined for 72 h at a specified time interval. The velocity of water vapor transmission (WVTR; $g \times m^{-2} \times s^{-1}$) was calculated from the slope of the regression curve of the transmitted moisture content from the film versus of the time. Then, WVTR was used for the calculation of WVP according to the following equations [5]:

$$J = VTR = \frac{\Delta W/\Delta t}{A} \quad (2)$$

$$WVP = \frac{WVTR}{p(R1 - R2)} \times X \quad (3)$$

where, WVP ($g \times m^{-1} \times s^{-1} \times Pa^{-1}$), A is the film's area (m^2), x is the film thickness (m), and ΔP is the pressure difference between the inner and outer surfaces of the film in vials (ΔP = 3169 Pa).

Color Measurement

To determine the surface color of the film samples, the CIE (Minolta CR300 158 Series, Minolta Camera Co. Ltd., Osaka, Japan) was used. The bright-dark (L*), green–red (a*) and blue-yellow (b*) of films were recorded [20].

Water Contact Angle (WCA) Measurement

The WCA was determined by the sessile drop method. Firstly, a drop of distilled water was placed on the surface of the samples using a syringe and imaged using a camera (Canon MV50, Taiwan) with × 6 magnification at the initial exposure time (t_1) and 60 s after the droplet contact angle (t_2). The angle between the tangent line at the point of contact and the line drawn along the film surface was measured as the WCA.

Determination of Mechanical Properties

The ultimate tensile strength (UTS) and strain to break (STB) of films were measured by Gotech-AI-7000M according to ASTM D882-95. Film samples were cut in 0/5 × 8 cm and conditioned for 24 h at a relative humidity of 55(calcium nitrate) and ambient temperature. The initial distance between the two jaws and the speed of the jaws was 50 mm and 5 mm/min, respectively [1].

Scanning Electron Microscopy (SEM)

The surface morphology of films was studied using a SEM (Leo 1450 VP, Germany). Due to the insulation of films, the samples were covered with gold and platinum using the Polisher Model SC-7620.

Differential Scanning Calorimetry (DSC)

The DSC test (DSC400, SANAF, Iran) was performed to analysis the thermal properties of the film samples. A 20 ± 5 mg of each film sample was placed in sample pan and an empty pan was used as a reference. The glass transition temperature (T_g) and melting temperature (T_m) of the samples were recorded by scanning from 25 to 250 °C with a heating rate of 10 °C min^{-1}.

Fourier Transforms Infrared (FT-IR) Spectroscopy

The structure interactions in the nanocomposite film samples were investigated with FT-IR spectroscopy (Tensor27, Bruker, Germany). The spectra were collected over the

wavenumber range of 4000–400 cm^{-1}. The KBr- pellet method was used for sample preparation.

X-ray Diffraction (XRD) Analyses

X-ray diffraction test was used to study the crystalline structure of the nanocomposite films. To perform the test, the X-ray diffractometer (Kristalloflex D500, Siemens, Germany) was set at 40 kV and 40 mA, and the samples were exposed to the X-ray with a wavelength of 0.1539 nm. Refractive radiation from the sample at ambient temperature and in the range of (2θ) from 2° to 70° was recorded. The speed of the test was 1° and the step size was 0.02.

Antibacterial Activity

The inhibition activity of the film samples against *Pseudomonas aeruginosa DSM 101013*, *Salmonella typhimurium DSM 101475*, *Staphylococcus aureus* DSM 102265, and *Escherichia coli* DSM 101124 was studied using the disc diffusion method. Firstly, the bacteria suspensions (1.5×10^8 CFU/mL) were prepared and cultured on surface of prepared Mueller Hinton Agar plate. The film samples were prepared as form round discs with 12 mm diameter. Then, the samples were put on the surface of Mueller Hinton agar plates and were incubated at 37 °C for 24 h. After that, the diameter of the inhibition zones around the film samples were measured in triplicate by the caliper and the means were reported [1].

Statistical Analysis Statistical analysis was conducted based on completely randomized design (one-way) ANOVA with SPSS 20 software (IBM Corporation, Armonk, NY, USA). Significant differences between treatments were estimated using Duncan test.

Results and Discussion

Fourier Transforms Infrared (FT-IR)

The FT-IR spectrum of neat gelatin, pure β-glucan, G/βG20%, G/ZnONPs5%, G/βG20%/ZnONPs2.5%, and G/βG20%/ZnONPs5% film samples are shown in Fig. 1. In the spectrum of neat gelatin film, the absorption peaks were observed at 3842, 3740, and 3626 cm^{-1}. The peaks observed in the first two waves were related to C-H tensile vibrations, nitrogen- hydrogen bonding bonds depending on the number of crosslinks, and asymmetric O–H tensile strengths in the combination; also, robust absorption was observed at 1689 and 1531 cm^{-1} waves. The FTIR spectrum for pure β-glucan showed a broad and strong peak at 3419 cm^{-1}, related to the tensile bond of OH (RCH_2OH) and the nitrogen–hydrogen bond (NH). Moreover, the observed peak at 2926 cm^{-1} was associated with the tensile vibrations of the CH methyl group. As shown in Fig. 1, the addition of 20% β-glucan in the gelatin film caused changes in the spectrum. The peaks observed at wavelengths 3840, 3736, and 3623 cm^{-1}, related to free hydroxyl bonds (OH), were bound to the phenolic ring present in gelatin and β-glucan; the combination of the two substances did not show a significant change in the area. Furthermore, by adding 5% ZnONPs in the gelatin-based film, the peaks observed at 3840, 3736, 3623, 1688, 1529, 954, and 679 cm^{-1} did not change the gelatin index

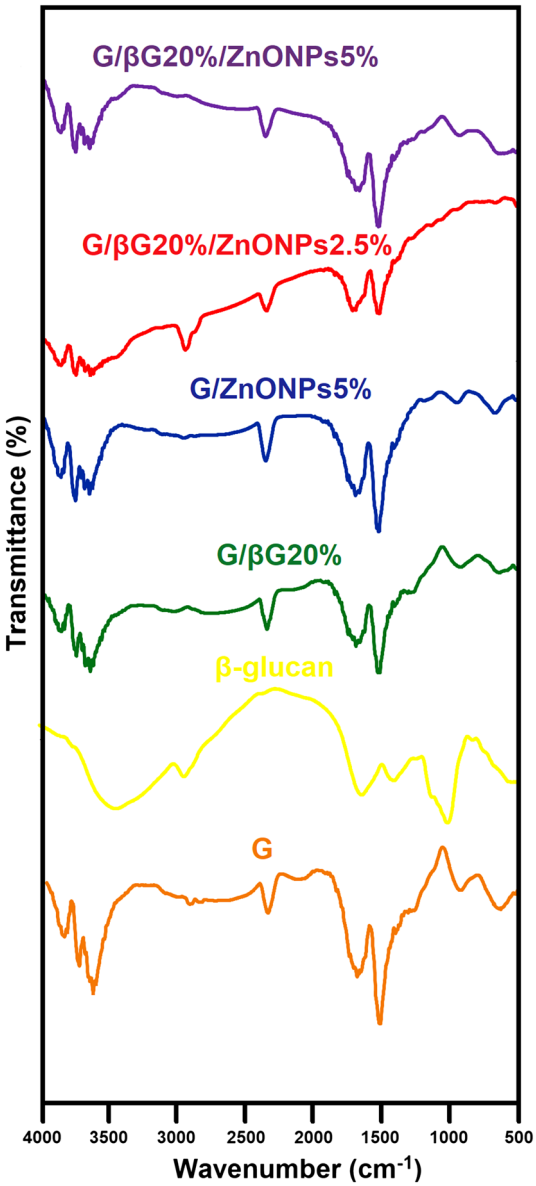

Fig. 1 Fourier transforms infrared (FT-IR) spectra of neat gelatin film, pure β-glucan, and G/βG20%, G/ZnONPs5%, G/βG20%/ZnONPs2.5%, and G/βG20%/ZnONPs5% film samples. *G* gelatin, *βG* β-glucan, *ZnONPs* zinc oxide nanoparticles

significantly. In Fig. 4, the observed peaks at 3439, 2930, 1280, 1140, 1072, 582, and 520 cm^{-1} indicate the presence of β-glucan, while the peaks corresponding to the wavenumbers 1193 cm^{-1} indicate the presence of ZnONPs (2.5%). By increasing the concentration of ZnONPs to 5%, the peak was observed at 2830 and 2862 cm^{-1} with a small amount, and a very wide peak was transferred to the wavelength of 3008 cm^{-1}, indicating an increase in hydroxyl groups. As seen in Fig. 4, increasing concentrations of β-glucan and ZnONPs did not change the FT-IR spectrum of neat gelatin film, and all spectral components of its main constituent elements were visible. These findings were in line with the reported results by Nagaraju et al. [21] and Sinha et al. [22].

Moisture Absorption

Moisture absorption is an essential parameter in evaluating the water barrier properties of packaging films. The results of the moisture absorption values of film samples are presented in Table 2. The neat gelation film showed the highest moisture absorption (35.72 ± 0.93%) related to the gelatin hydrophilic nature. The addition of β-glucan to the gelatin-based films significantly ($p < 0.05$) decreased the moisture absorption. This reduction could be described by the interaction between gelatin and β-glucan, creating a strong structure. Moreover, the incorporation of ZnONPs in the gelatin-based films caused a reduction in moisture absorption values, higher than the reduction effect of β-glucan. The lowest water absorption value (28.01 ± 1.59%) was attributed to the G/βG20%/ZnONPs5% sample. The decrease in moisture absorption by the incorporation of ZnONPs could be explained by increasing crosslinking between gelatin chains and reducting chain mobility due to filling the free spaces in the gelatin matrix. Similar results were reported by previous studies [4, 5].

Water Vapor Permeability (WVP)

WVP of films is another important factor affecting their water barrier properties. The WVP values of film samples are provided in Table 2. The neat gelatin film showed the highest WVP value (2.15×10^{-8} $g.m^{-1}.h^{-1}.Pa^{-1}$) compared to other films, due to its inherent hydrophilicity [23]. As a result, the addition of β-glucan and ZnONPs to the film matrix significantly ($p < 0.05$) decreased WVP values of the gelatin-based films. In this regard, G/βG20%/ZnONPs5% film sample showed the lowest WVP with a value of 1.58×10^{-8} g m^{-1} h^{-1} Pa^{-1}. According to previous literature [8, 11], the reduction in WVP by the addition of β-glucan and ZnONPs could be attributed to the increase in interactions between gelatin chains, making the diffusion path more tortuous and decreasing the diffusion rate of water vapor through the films.

Water Contact Angle Analysis (WCA)

WCA measurement provides information on the surface hydrophobicity of films [24]. Table 2 presents the WCA values of the film samples. The surface wettability and contact angle measurements are related to each other; low surface wettability leads to high contact angle and vice versa [15]. Among the film samples, the neat gelatin one exhibited the lowest contact angle (44°), indicating a high surface wettability due to the gelatin hydrophilic nature. A similar observation was also reported by Nafchi et al. [25]. The WCA values of films showed an increasing trend by adding β-glucan and ZnONPs and increasing their concentrations. Thus, the highest WCA value was associated with G/βG20%/ZnONPs5% sample with a value of53°. In line with these results, Amjadi et al. [2] reported that the incorporation of ZnONPs in the gelatin-based films increased WCA due to:

Table 2 Water barrier properties of gelatin-based film samples

Samples	Moisture absorption (%)	WVP ($\times 10^{-8}$ $g.m^{-1}.h^{-1}.Pa^{-1}$)	WCA (°)	
			t_1	t_2
G	35.72 ± 0.93^{a}	2.15 ± 1.82^{a}	44.29 ± 0.73^{e}	44.29 ± 0.73^{d}
G/βG10%	32.88 ± 1.08^{bc}	1.93 ± 2.01^{c}	49.89 ± 1.40^{bc}	47.77 ± 0.85^{bc}
G/βG20%	34.10 ± 2.58^{ab}	1.96 ± 7.31^{bc}	$49.\ 03 \pm 1.27^{cd}$	$49.\ 03 \pm 1.27^{b}$
G/ZnONPs2.5%	31.79 ± 1.22^{bc}	2.03 ± 1.98^{b}	46.83 ± 0.33^{d}	46.83 ± 0.33^{c}
G/βG10%/ZnONPs2.5%	30.28 ± 1.50^{cd}	2.01 ± 1.21^{bc}	47.55 ± 2.21^{cd}	49.07 ± 0.73^{b}
G/βG20%/ZnONPs2.5%	30.30 ± 0.82^{cd}	1.85 ± 4.72^{d}	49.14 ± 0.52^{cd}	49.51 ± 1.14^{b}
G/ZnONPs5%	28.87 ± 1.45^{d}	1.70 ± 1.09^{e}	53.06 ± 1.45^{ab}	52.06 ± 1.45^{a}
G/βG10%/ZnONPs5%	28.62 ± 1.50^{d}	1.62 ± 3.22^{ef}	53.08 ± 1.75^{a}	52.06 ± 0.82^{a}
G/βG20%/ZnONPs5%	28.01 ± 1.59^{d}	1.58 ± 3.66^{g}	53.56 ± 1.05^{a}	53.08 ± 1.75^{a}

Data are expressed as mean ± standard deviation (n = 3) and different letters show significant difference at the 5% level in Duncan's test ($p < 0.05$)

WVP water vapor permeability, *WCA* water contact angle at the initial exposure time (t_1) and 60 s after the droplet contact angle (t_2), *G* gelatin, *βG* β-glucan, *ZnONPs* zinc oxide nanoparticles

(a) the formation of hydrogen bonds between gelatin and ZnONPs that leads to the reduction of the free hydrophilic groups in the gelatin structure; (b) the increase in the crystallinity and compactness of polymer chains by the incorporation of ZnO NPs. Moreover, the increase in WCA by incorporating ZnONPs in the chitosan [15], agar, carrageenan, and CMC-based films [26] was reported by previous studies.

Surface Color of the Films

The results of color measurement are provided in Table 3. As observed, the neat gelatin film showed a clear and yellowish appearance. The color parameters of composite film samples exhibited a significant difference with those of neat gelatin films. The L* parameter was decreased by increasing the concentrations of β-glucan and ZnONPs. Similar results were observed in previous studies for ZnONPs incorporated gelatin [5, 27] and chitosan-based films [28]. The cloudy film at high concentrations of ZnONPs could be attributed to the accumulation of ZnONPs in the film matrix, located between the polymer chains. This phenomenon can be useful for food packaging sensitive to light with a need for opaque coatings. The a* parameter, showed the greenness-redness of the samples. As observed, by increasing concentrations of β-glucan and ZnONPs, the a* parameter showed negative values, i.e., the color of the samples tended to be green. Furthermore, the b* parameter, representing the yellowness-blueness of the samples, showed that the color of the films tended to be yellow by increasing the concentration of β-glucan and ZnONPs.

Table 3 Color parameters of gelatin-based film samples

Samples	L*	a*	b*
G	64.8 ± 0.10^{a}	3.53 ± 11.72^{a}	19.13 ± 0.41^{d}
G/βG10%	49.89 ± 0.05^{c}	-11.36 ± 0.25^{b}	13.60 ± 0.20^{g}
G/βG20%	49.03 ± 1.27^{c}	-13.91 ± 0.27^{b}	18.10 ± 0.17^{e}
G/ZnONPs2.5%	46.83 ± 0.33^{d}	-9.33 ± 0.30^{b}	15.00 ± 0.40^{b}
G/βG10%/ ZnONPs2.5%	47.55 ± 2.21^{cd}	-14.16 ± 0.20^{b}	27.06 ± 0.30^{f}
G/βG20%/ ZnONPs2.5%	49.14 ± 0.52^{c}	-7.40 ± 0.34^{b}	30.93 ± 0.41^{a}
G/ZnONPs5%	53.06 ± 1.45^{b}	-11.43 ± 0.35^{b}	7.86 ± 0.29^{c}
G/βG10%/ ZnONPs5%	53.08 ± 1.75^{b}	-14.33 ± 0.20^{b}	22.56 ± 0.51^{h}
G/βG20%/ ZnONPs5%	53.56 ± 1.05^{b}	-11.16 ± 0.29^{b}	28.03 ± 0.25^{b}

Data are expressed as mean ± standard deviation (n = 3) and different letters show significant difference at the 5% level in Duncan's test ($p < 0.05$)

G gelatin, *βG* β-glucan, *ZnONPs* zinc oxide nanoparticles

Thickness and Mechanical Properties of Films

Figure 2 shows the thickness values and mechanical properties of the film samples. As seen (Fig. 2a), the thickness values of film samples were increased by the addition of β-glucan and ZnONPs. Thus the highest thickness value was related to G/βG20%/ZnONPs5% sample; this finding could be attributed to the changes in dry matter content and gelatin matrix structure. Similar results were reported by Jahed et al. [29]. As shown in Fig. 2b, the UTS values of film samples showed no significant difference by adding β-glucan. However, the incorporation of ZnONPs significantly increased the UTS values of the samples. The UTS values of film samples containing ZnONPs and β-glucan exhibited no significant difference compared with the neat gelatin films. Furthermore, the STB value of film samples was significantly increased by adding 20% β-glucan (Fig. 2c). However, the addition of ZnONPs significantly decreased the STB values of film samples. The mechanical properties of films depend on the interactions between the polymer chains in

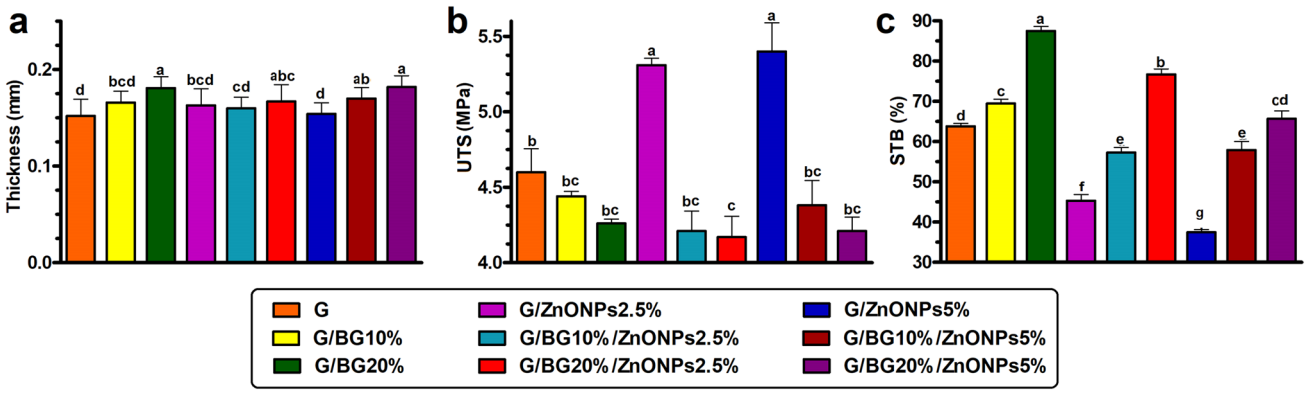

Fig. 2 Thickness (**a**), ultimate tensile strength (UTS) (**b**) and strain to break (STB) (**c**) profiles of gelatin-based film samples. Data are expressed as mean ± standard deviation (n = 3) and different letters show significant difference at the 5% level in Duncan's test ($p < 0.05$). *G* gelatin, *βG* β-glucan, *ZnONPs* zinc oxide nanoparticles

the film matrix [30]. In this regard, the effect of ZnONPs on the mechanical properties of film samples can be explained by interactions between ZnONPs and the gelatin matrix to obtain a stiff continuous network and reduce the mobility of the polymer chains. Many studies have reported that the incorporation of ZnONPs improves the mechanical properties of gelatin-based films [2, 31, 32].

X-Ray Diffraction (XRD) Analyses

The XRD diffractograms of neat gelatin, G/βG20%, G/βG20%/ZnONPs2.5%, and G/ZnONPs5% film samples are shown in Fig. 3. The diffractogram of neat gelatin film exhibited two specific peaks near 2θ of 23° and 45°, indicating that this film had a semi-crystalline structure. Similar results were reported in previous studies [1]. The XRD pattern of the G/βG20% sample showed three peaks at 2θ of 20°, 36°, and 40°, while the pattern of the G/βG20%/ZnONPs2.5% sample exhibited four peaks at 2θ of 21°, 31°, 34°, and 38. Additionally, the X-ray diffraction pattern of G/ZnONPs5% showed the decreased intensity of all peaks compared with other samples, indicating the formation of a composite structure by incorporating ZnONPs.

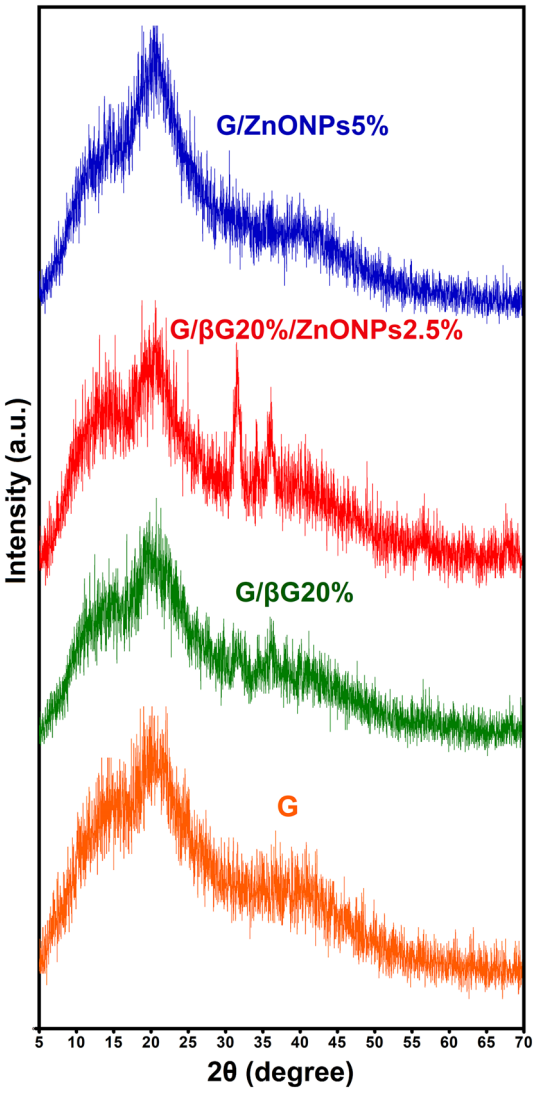

Fig. 3 X-ray diffraction (XRD) patterns of neat gelatin, G/βG20%, G/βG20%/ZnONPs2.5%, and G/ZnONPs5% film samples. *G* gelatin, *βG* β-glucan, *ZnONPs* zinc oxide nanoparticles

Differential Scanning Calorimetry (DSC)

The thermal properties of film samples were assessed by DSC analyses; the obtained results, including glass transition temperature (T_g) and melting temperature (T_m) of film samples, are given in Table 4. The neat gelatin film showed a glass transition at 63.4 °C, consistent with previous reports [33]. The addition of the 20% w/v of β-glucan without ZnO decreased T_g; however, the addition of 5% of ZnONPs increased T_g, indicating the desired effect of this nanofiller on gelatin amorphous regions, i.e., reducing the mobility of chains. The reduction effect of β-glucan on T_g is such that even in films, which use β-glucan with ZnONPs, T_g is slightly lower than the other films. However, the addition of ZnONPs (2.5% and 5%) and β-glucan (10% and 20%) significantly increased T_m. According to previous literature, this phenomenon can be attributed to the interactions between gelatin, ZnONPs, and β-glucan, as well as the formation of dense crystalline regions in the biopolymer matrix [34, 35].

Scanning Electron Microscopy (SEM)

The SEM images of film samples are shown in Fig. 4. As observed in Fig. 4A and 4a, the neat gelatin film exhibited a flat surface and a uniform composition of the structure. The SEM images of G/βG20% (Fig. 4B and 4b) showed small pellets relatively uniformly dispersed in the matrix. This β-Glucan granular structure has been recently reported [36]. In the SEM images of G/βG20%/ZnONPs2.5% (Fig. 4C and 4c) and G/βG20%/ZnONPs5% (Fig. 4D and 4d), the flat gelatin background with diffused β-Glucan particles is clearly visible. Moreover, ZnONPs appear as fine white particles

Table 4 Thermal Properties of gelatin-based film samples

Samples	T_g (°C)	T_m (°C)
G	63.4	70.9
G/βG20%	54.1	78.1
G/βG10%/ZnONPs2.5%	45.9	100.2
G/ZnONPs5%	64.2	78.0
G/βG20%/ZnONPs5%	49.3	82.1

T_g glass transition temperature and T_m melting temperature; *G*: gelatin; *βG* β-glucan and *ZnONPs* zinc oxide nanoparticles

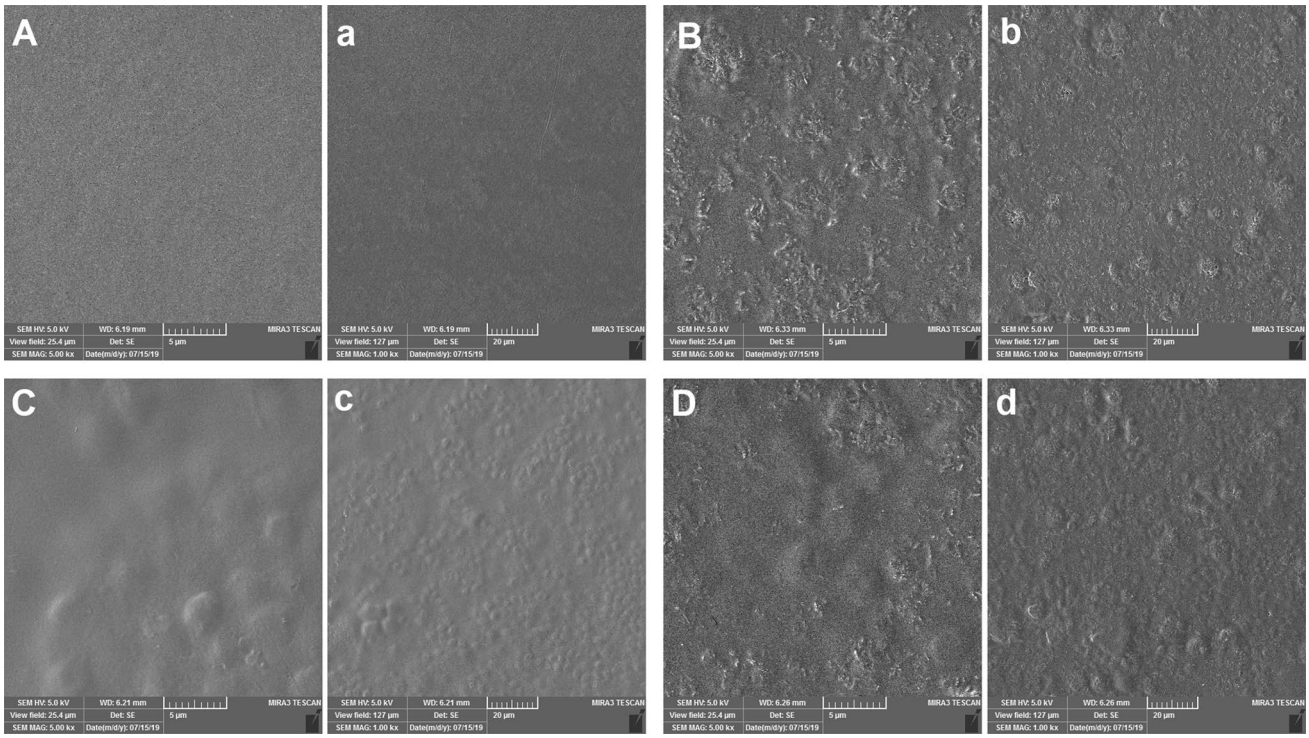

Fig. 4 Scanning electron microscopy (SEM) images of the surface of neat gelatin (**A** and **a**), G/βG20% (**B** and **b**), G/βG20%/ZnONPs2.5% (**C** and **c**), and G/βG20%/ZnONPs5% (**D** and **d**) film samples. *G* gelatin, *βG* β-glucan, *ZnONPs* zinc oxide nanoparticles

in the gelatin matrix, the sample containing 2.5% agglomerated in some places as a mass. This state is observed in the G/βG20%/ZnONPs2.5% sample, in which the amount of dispersed particles is higher than the G/βG20%/ZnONPs5% sample. These results are in line with those of previous studies [37–39].

Antibacterial Activity

The inhibition activity of the ZnONPs incorporated film samples against *P. aeruginosa*, *S. typhimurium*, *S. aureus,* and *E. coli* bacteria are summarized in Table 5. According to the table, the incorporation of ZnONPs provided inhibition activity against all investigated bacteria. Additionally, the increase in the concentration of ZnONPs significantly enhanced the antibacterial activity of the film samples. This activity can be described with two mechanisms of (1) penetration of the released Zn^{2+} ions by ZnONPs into the bacterial cell membrane, reacting with cytoplasmic content to kill bacteria, (2) producing reactive oxygen species (ROS) by ZnONPs, damaging the bacterial lipids, proteins, and DNA [2]. The combination of ZnONPs with β-glucan in the gelatin-based film significantly decreased the antibacterial activity against all investigated bacteria. However, the increase in β-glucan concentration caused no significant difference in the antibacterial activity of ZnONPs incorporated films.

Table 5 Antibacterial activity of gelatin-based film samples

Samples	Inhibitory zone (mm)			
	P. aeruginosa	*S. typhimorium*	*S. aureus*	*E. coli*
G/ZnONPs2.5%	13.5 ± 1.04^{c}	13.0 ± 1.74^{b}	15.0 ± 1.13^{d}	13.0 ± 1.25^{d}
G/βG10%/ZnONPs2.5%	13.0 ± 1.20^{d}	12.0 ± 1.55^{c}	16.0 ± 1.23^{c}	12.0 ± 1.36^{e}
G/βG20%/ZnONPs2.5%	13.0 ± 2.01^{d}	12.0 ± 2.05^{c}	15.7 ± 1.48^{c}	12.2 ± 1.19^{e}
G/ZnONPs5%	16.2 ± 1.13^{a}	16.2 ± 1.90^{a}	18.0 ± 1.53^{a}	15.7 ± 1.34^{a}
G/βG10%/ZnONPs5%	14.0 ± 2.10^{b}	13.0 ± 1.48^{b}	16.7 ± 1.81^{b}	13.7 ± 1.78^{c}
G/βG20%/ZnONPs5%	14.2 ± 1.32^{b}	13.2 ± 1.72^{b}	17.0 ± 2.10^{b}	15.0 ± 1.52^{b}

Data are expressed as mean ± standard deviation (n = 3) and different letters show significant difference at the 5% level in Duncan's test ($p < 0.05$); *G* gelatin; *βG* β-glucan and *ZnONPs* zinc oxide nanoparticles

Furthermore, the results showed that the highest inhibition activity of all film samples was against *S. aureus* bacteria, indicating that the antibacterial activity of the ZnONPs-incorporated films against gram-positive bacteria was higher than that against gram-negative bacteria. This finding was in line with those reported by previous studies [4, 27]. According to these studies, this phenomenon is related to the structural differences in the outer membrane of these bacteria. Therefore, the gram-negative bacteria have a complex cell wall composed of a thin peptidoglycan layer and an outer membrane; this complex cell wall reduces the permeability of the produced ROS and Zn^{2+} ions by ZnONPs into the bacterial cell.

Conclusion

The ZnONPs incorporated gelatin/β-glucan nanocomposite films were successfully developed with satisfactory features. The incorporation of ZnONPs and β-glucan improved the mechanical properties of gelatin-based films. Moreover, the water barrier properties of film samples significantly were improved by increasing ZnONPs concentration. The results of XRD, DSC, SEM, and FT-IR analyses showed that the incorporation of ZnONPs and β-glucan had no adverse effect on the morphological and thermal properties and the crystallinity of gelatin-based films. The ZnONPs incorporated film samples, especially those with high concentrations of ZnONPs, exhibited inhibition activity against *P. aeruginosa*, *S. typhimurium*, *S. aureus,* and *E. coli* bacteria. These findings showed that the ZnONPs incorporated gelatin/β-glucan nanocomposite films had suitable physicochemical properties and biological activity to be applied as an active packaging system.

Acknowledgment The authors gratefully acknowledge the supports of the Islamic Azad University of Tabriz. This research did not receive any specific grant from funding agencies in public, commercial, or non-profit sectors.

Compliance with Ethical Standards

Conflict of interest The author(s) declared no potential conflicts of interest with respect to the research, authorship, and/or publication of this article.

References

1. Karimi N, Alizadeh A, Almasi H, Hanifian S (2020) Preparation and characterization of whey protein isolate/polydextrose-based nanocomposite film incorporated with cellulose nanofiber and *L. plantarum*: a new probiotic active packaging system. LWT. https://doi.org/10.1016/j.lwt.2019.108978
2. Amjadi S, Nazari M, Alizadeh SA, Hamishehkar H (2020) Multifunctional betanin nanoliposomes-incorporated gelatin/chitosan nanofiber/ZnO nanoparticles nanocomposite film for fresh beef preservation. Meat Sci. https://doi.org/10.1016/j.meatsci.2020.108161
3. Pirsa S, Farshchi E, Roufegarinejad L (2020) Antioxidant/antimicrobial film based on carboxymethyl cellulose/gelatin/TiO_2–Ag nano-composite. J Polym Environ 28(12):3154–3163
4. Shahmohammadi Jebel F, Almasi H (2016) Morphological, physical, antimicrobial and release properties of ZnO nanoparticles-loaded bacterial cellulose films. Carbohydr Polym 149:8–19. https://doi.org/10.1016/j.carbpol.2016.04.089
5. Amjadi S, Emaminia S, Davudian SH et al (2019) Preparation and characterization of gelatin-based nanocomposite containing chitosan nanofiber and ZnO nanoparticles. Carbohydr Polym. https://doi.org/10.1016/j.carbpol.2019.03.062
6. Poverenov E, Rutenberg R, Danino S et al (2014) Gelatin-chitosan composite films and edible coatings to enhance the quality of food products: layer-by-layer vs. blended formulations. Food Bioprocess Technol 7:3319–3327
7. Amjadi S, Emaminia S, Nazari M et al (2019) Application of reinforced ZnO nanoparticle-incorporated gelatin bionanocomposite film with chitosan nanofiber for packaging of chicken fillet and cheese as food models. Food Bioprocess Technol 12:1205–1219
8. Razzaq HAA, Pezzuto M, Santagata G et al (2016) Barley β-glucan-protein based bioplastic film with enhanced physicochemical properties for packaging. Food Hydrocoll 58:276–283. https://doi.org/10.1016/j.foodhyd.2016.03.003
9. Ali U, Bijalwan V, Basu S et al (2017) Effect of β-glucan-fatty acid esters on microstructure and physical properties of wheat straw arabinoxylan films. Carbohydr Polym 161:90–98. https://doi.org/10.1016/j.carbpol.2016.12.036
10. Chang J, Li W, Liu Q et al (2019) Preparation, properties, and structural characterization of β-glucan/pullulan blend films. Int J Biol Macromol 140:1269–1276. https://doi.org/10.1016/j.ijbiomac.2019.08.208
11. Noshirvani N, Ghanbarzadeh B, Rezaei Mokarram R, Hashemi M (2017) Novel active packaging based on carboxymethyl cellulose-chitosan-ZnO NPs nanocomposite for increasing the shelf life of bread. Food Packag Shelf Life 11:106–114. https://doi.org/10.1016/j.fpsl.2017.01.010
12. Marra A, Silvestre C, Duraccio D, Cimmino S (2016) Polylactic acid/zinc oxide biocomposite films for food packaging application. Int J Biol Macromol 88:254–262. https://doi.org/10.1016/j.ijbiomac.2016.03.039
13. Espitia PJP, de Soares NFF, dos ReisCoimbra JS et al (2012) Zinc oxide nanoparticles: synthesis, antimicrobial activity and food packaging applications. Food Bioprocess Technol 5:1447–1464
14. Al-Naamani L, Dobretsov S, Dutta J (2016) Chitosan-zinc oxide nanoparticle composite coating for active food packaging applications. Innov Food Sci Emerg Technol 38:231–237. https://doi.org/10.1016/j.ifset.2016.10.010
15. Matai I, Sachdev A, Dubey P et al (2014) Antibacterial activity and mechanism of Ag-ZnO nanocomposite on *S. aureus* and GFP-expressing antibiotic resistant *E. coli*. Colloids Surf B 115:359–367. https://doi.org/10.1016/j.colsurfb.2013.12.005
16. Silvestre C, Cimmino S, Pezzuto M et al (2013) Preparation and characterization of isotactic polypropylene/zinc oxide microcomposites with antibacterial activity. Polym J 45:938–945. https://doi.org/10.1038/pj.2013.8
17. Gómez-Estaca J, Bravo L, Gómez-Guillén MC et al (2009) Antioxidant properties of tuna-skin and bovine-hide gelatin films induced by the addition of oregano and rosemary extracts. Food Chem 112:18–25. https://doi.org/10.1016/j.foodchem.2008.05.034

18. Zabihollahi N, Alizadeh A, Almasi H, et al (2020) Development and characterization of carboxymethyl cellulose based probiotic nanocomposite film containing cellulose nanofiber and inulin for chicken fillet shelf life extension. Int J Biol Macromol
19. Neus Angles M, Dufresne A (2000) Plasticized starch/tuniein whiskers nanocomposites. 1. Structural analysis. Macromolecules 33:8344–8353. https://doi.org/10.1021/ma0008701
20. Amjadi S, Nouri S, Yorghanlou RA, Roufegarinejad L (2020) Development of hydroxypropyl methylcellulose/sodium alginate blend active film incorporated with *Dracocephalum moldavica* L. essential oil for food preservation. J Thermoplast Compos Mater 0892705720962153
21. Nagaraju G, Udayabhanu S et al (2017) Electrochemical heavy metal detection, photocatalytic, photoluminescence, biodiesel production and antibacterial activities of Ag–ZnO nanomaterial. Mater Res Bull 94:54–63. https://doi.org/10.1016/j.materresbull.2017.05.043
22. Sinha D, De D, Ayaz A (2018) Performance and stability analysis of curcumin dye as a photo sensitizer used in nanostructured ZnO based DSSC. Spectrochim Acta Part A 193:467–474. https://doi.org/10.1016/j.saa.2017.12.058
23. Sanuja S, Agalya A, Umapathy MJ (2015) Synthesis and characterization of zinc oxide-neem oil-chitosan bionanocomposite for food packaging application. Int J Biol Macromol 74:76–84. https://doi.org/10.1016/j.ijbiomac.2014.11.036
24. Kaya M, Khadem S, Cakmak YS et al (2018) Antioxidative and antimicrobial edible chitosan films blended with stem, leaf and seed extracts of Pistacia terebinthus for active food packaging. RSC Adv 8:3941–3950. https://doi.org/10.1039/c7ra12070b
25. Nafchi AM, Alias AK, Mahmud S, Robal M (2012) Antimicrobial, rheological, and physicochemical properties of sago starch films filled with nanorod-rich zinc oxide. J Food Eng 113:511–519. https://doi.org/10.1016/j.jfoodeng.2012.07.017
26. Kanmani P, Rhim JW (2014) Properties and characterization of bionanocomposite films prepared with various biopolymers and ZnO nanoparticles. Carbohydr Polym 106:190–199. https://doi.org/10.1016/j.carbpol.2014.02.007
27. Shankar S, Teng X, Li G, Rhim JW (2015) Preparation, characterization, and antimicrobial activity of gelatin/ZnO nanocomposite films. Food Hydrocoll 45:264–271. https://doi.org/10.1016/j.foodhyd.2014.12.001
28. Jouki M, Yazdi FT, Mortazavi SA, Koocheki A (2014) Quince seed mucilage films incorporated with oregano essential oil: Physical, thermal, barrier, antioxidant and antibacterial properties. Food Hydrocoll 36:9–19. https://doi.org/10.1016/j.foodhyd.2013.08.030
29. Jahed E, Khaledabad MA, Bari MR, Almasi H (2017) Effect of cellulose and lignocellulose nanofibers on the properties of *Origanum vulgare* ssp. gracile essential oil-loaded chitosan films. React Funct Polym 117:70–80. https://doi.org/10.1016/j.reactfunctpolym.2017.06.008
30. Sahraee S, Ghanbarzadeh B, Milani JM, Hamishehkar H (2017) Development of gelatin bionanocomposite films containing chitin and ZnO nanoparticles. Food Bioprocess Technol 10:1441–1453. https://doi.org/10.1007/s11947-017-1907-2
31. Mohammadi H, Kamkar A, Misaghi A (2018) Nanocomposite films based on CMC, okra mucilage and ZnO nanoparticles: physico mechanical and antibacterial properties. Carbohydr Polym 181:351–357. https://doi.org/10.1016/j.carbpol.2017.10.045
32. Oun AA, Rhim JW (2017) Preparation of multifunctional chitin nanowhiskers/ZnO-Ag NPs and their effect on the properties of carboxymethyl cellulose-based nanocomposite film. Carbohydr Polym 169:467–479. https://doi.org/10.1016/j.carbpol.2017.04.042
33. Mukherjee I, Rosolen M (2013) Thermal transitions of gelatin evaluated using DSC sample pans of various seal integrities. J Therm Anal Calorim 114:1161–1166. https://doi.org/10.1007/s10973-013-3166-4
34. Veverka M, Dubaj T, Gallovič J et al (2014) Beta-glucan complexes with selected nutraceuticals: synthesis, characterization, and stability. J Funct Foods 8:309–318. https://doi.org/10.1016/j.jff.2014.03.032
35. Nováka M, Synytsyaa A, Gedeonb O et al (2012) Yeast β(1–3), (1–6)-d-glucan films: preparation and characterization of some structural and physical properties. Carbohydr Polym 87:2496–2504. https://doi.org/10.1016/j.carbpol.2011.11.031
36. Limberger-Bayer VM, de Francisco A, Chan A et al (2014) Barley β-glucans extraction and partial characterization. Food Chem 154:84–89
37. Xiong G, Pal U, Serrano JG et al (2006) Photoluminescence and FTIR study of ZnO nanoparticles: the impurity and defect perspective. Phys Status Solidi Curr Top Solid State Phys 3:3577–3581. https://doi.org/10.1002/pssc.200672164
38. Handore K, Bhavsar S, Horne A et al (2014) Novel green route of synthesis of ZnO nanoparticles by using natural biodegradable polymer and its application as a catalyst for oxidation of aldehydes. J Macromol Sci Part A 51:941–947. https://doi.org/10.1080/10601325.2014.967078
39. Rokesh K, Nithya A, Jeganathan K, Jothivenkatachalam K (2016) A Facile solid state synthesis of cone-like ZnO microstructure an efficient solar-light driven photocatalyst for rhodamine B degradation. Mater Today Proc 3:4163–4172. https://doi.org/10.1016/j.matpr.2016.11.091

Affiliations

Shahin Sherafatkhah Azari[1] · Ainaz Alizadeh[1] · Leila Roufegarinejad[1] · Narmela Asefi[1] · Hamed Hamishehkar[2]

✉ Ainaz Alizadeh
ainaz_alizadeh@hotmail.com; a.alizadeh@iaut.ac.ir

[1] Department of Food Science and Technology, Tabriz Branch, Islamic Azad University, Tabriz, Iran

[2] Drug Applied Research Center, Tabriz University of Medical Sciences, Tabriz, Iran